Symplectic methods for the Ablowitz–Ladik discrete nonlinear Schrödinger equation

2007 J. Phys. A: Math. Theor. 40 2425

(http://iopscience.iop.org/1751-8121/40/10/012)

J. Phys. A: Math. Theor. **40** (2007) 2425–2437 doi:10.1088/1751-8113/40/10/012

Symplectic methods for the Ablowitz–Ladik discrete nonlinear Schrödinger equation

Yifa Tang[1], **Jianwen Cao**[2], **Xiangtao Liu**[1] **and Yuanchang Sun**[1,3]

[1] LSEC, ICMSEC, Academy of Mathematics & Systems Science, Chinese Academy of Sciences, PO Box 2719, Beijing 100080, People's Republic of China
[2] Institute of Software, Chinese Academy of Sciences, Beijing 100080, People's Republic of China
[3] Graduate School of the Chinese Academy of Sciences, Beijing 100080, People's Republic of China

E-mail: tyf@lsec.cc.ac.cn

Received 18 July 2006, in final form 25 January 2007
Published 21 February 2007
Online at stacks.iop.org/JPhysA/40/2425

Abstract
Using several kinds of coordinate transformations, we standardize the noncanonical symplectic structure of the Ablowitz–Ladik model (A–L model) of nonlinear Schrödinger equation (NLSE), then we employ some symplectic scheme to simulate the solitons motion and test the evolution of the discrete invariants of the A–L model and also the conserved quantities of the original NLSE. In comparison with a higher order non-symplectic scheme applied directly to the A–L model, we show the overwhelming superiorities of the symplectic method. We also compare the implementation of the same symplectic scheme to different standardized Hamiltonian systems resulting from different coordinate transformations, and show that the symmetric coordinate transformation improves the numerical results obtained via the asymmetric one, in preserving the invariants of the A–L model and the original NLSE.

PACS numbers: 02.30.H, 02.60.J, 03.40.K

1. Introduction

We consider the nonlinear cubic Schrödinger equation (NLSE) with initial condition

$$\begin{cases} \mathrm{i}W_t + W_{xx} + a|W|^2 W = 0, \\ W(x,0) = W_0(x) \end{cases} \tag{1}$$

where $x \in \mathbb{R}, a > 0$ is a constant and $W(x,t)$ is a complex function. Different initial conditions $W_0(x)$ decide different motions. For example, some kind of $W_0(x)$ with $W_0(\pm\infty) = 0$ will produce bright solitons motion (see [5, 11]). It is known that NLSE (1) has an infinite number of conserved quantities such as the *charge*, the *momentum*, the

energy, ... We write the first six as follows (refer to Zakharov and Shabat [18]):

$$B_1 = \int_{-\infty}^{+\infty} |W|^2 \mathrm{d}x, \qquad B_2 = \int_{-\infty}^{+\infty} \left\{ W\frac{\mathrm{d}\overline{W}}{\mathrm{d}x} - \overline{W}\frac{\mathrm{d}W}{\mathrm{d}x} \right\} \mathrm{d}x,$$

$$B_3 = \int_{-\infty}^{+\infty} \left\{ 2\left|\frac{\mathrm{d}W}{\mathrm{d}x}\right|^2 - a|W|^4 \right\} \mathrm{d}x, \qquad B_4 = \int_{-\infty}^{+\infty} \left\{ 2\frac{\mathrm{d}\overline{W}}{\mathrm{d}x}\frac{\mathrm{d}^2W}{\mathrm{d}x^2} - 3a|W|^2\overline{W}\frac{\mathrm{d}W}{\mathrm{d}x} \right\} \mathrm{d}x,$$

$$B_5 = \int_{-\infty}^{+\infty} \left\{ 2\left|\frac{\mathrm{d}^2W}{\mathrm{d}x^2}\right|^2 - 6a|W|^2\left|\frac{\mathrm{d}W}{\mathrm{d}x}\right|^2 - a\left(\frac{\mathrm{d}|W|^2}{\mathrm{d}x}\right)^2 + a^2|W|^6 \right\} \mathrm{d}x,$$

$$B_6 = \int_{-\infty}^{+\infty} \left\{ 2\frac{\mathrm{d}^2\overline{W}}{\mathrm{d}x^2}\frac{\mathrm{d}^3W}{\mathrm{d}x^3} - 5a\left|\frac{\mathrm{d}W}{\mathrm{d}x}\right|^2\frac{\mathrm{d}|W|^2}{\mathrm{d}x} - 10a|W|^2\frac{\mathrm{d}\overline{W}}{\mathrm{d}x}\frac{\mathrm{d}^2W}{\mathrm{d}x^2} + 5a^2|W|^4\overline{W}\frac{\mathrm{d}W}{\mathrm{d}x} \right\} \mathrm{d}x$$

where $\overline{W}$ is the complex conjugation of W.

For equation (1), one popular spatial discretization model is

$$\mathrm{i}\frac{\mathrm{d}W_l}{\mathrm{d}t} + \frac{W_{l+1} - 2W_l + W_{l-1}}{h^2} + \frac{a}{2}|W_l|^2(W_{l+1} + W_{l-1}) = 0, \tag{2}$$

where h is the spatial step-size and $W_l(t) = W(lh, t), l = \ldots, -1, 0, 1, \ldots$. This discrete model is the well-known Ablowitz–Ladik model (A–L model). It is proven that the solution of the A–L model (2) converges to that of the original continuous NLSE (1) when $h \longrightarrow 0$ (see [16]). Equation (2) is a completely integrable system (see [1, 5, 9, 11]), but it has a noncanonical symplectic structure for which standard symplectic integrators are not applicable. Via the generating functions technique (see [10, 14]) or standardization of the noncanonical symplectic structure (see [16, 17]), people have already constructed symplectic numerical methods for the A–L model (2).

In this paper, we construct approximations of the first six conserved quantities of the original NLSE by using centred differences (section 2), and give an easy program for calculation of the first six discrete invariants of the A–L model (section 3), then provide three kinds of coordinate transformations to standardize the A–L model (section 4), and then use a second-order symplectic scheme to simulate the solitons motion and test the evolution of the discrete invariants of the A–L model and also the conserved quantities of the original NLSE, for two different standardized Hamiltonians obtained via symmetric and asymmetric coordinate transformations, in comparison with a third-order non-symplectic method applied directly to the A–L model (sections 5 and 6), finally give some concluding remarks in section 7.

2. Approximations of conserved quantities of NLSE

Utilizing centred difference

$$W_x(lh, t) = \frac{W_{l+1} - W_{l-1}}{2h},$$

$$W_{xx}(lh, t) = \frac{W_{l+1} - 2W_l + W_{l-1}}{h^2},$$

$$W_{xxx}(lh, t) = \frac{W_{l+2} - 2W_{l+1} + 2W_{l-1} - W_{l-2}}{2h^3},$$

we can approximate the conserved quantities $B_1, \ldots, B_6$ of the original NLSE (1) as follows:

$$F_1 = h\sum_l W_l\overline{W}_l, \qquad F_2 = \sum_l \{W_l\overline{W}_{l+1} - W_{l+1}\overline{W}_l\},$$

$$F_3 = \frac{1}{2h}\sum_l \{2|W_l|^2 - W_{l+1}\overline{W}_{l-1} - W_{l-1}\overline{W}_{l+1}\} - ah\sum_l |W_l|^4,$$

$$\cdots\cdots\cdots\cdots$$

We will test the evolution of $F_m = FR_m + \mathrm{i}FI_m$ (FR_m and FI_m are the real part and imaginary part of F_m respectively), $1 \leqslant m \leqslant 6$ during numerical simulations in section 6.

3. Discrete invariants of Ablowitz–Ladik model

With the scaling transformations $X_l = \sqrt{\frac{ah^2}{2}}W_l$, $l = \ldots, -1, 0, 1, \ldots$; $s = -\frac{1}{h^2}t$, we change (2) into

$$\mathrm{i}\frac{\mathrm{d}X_l}{\mathrm{d}s} = X_{l+1} - 2X_l + X_{l-1} + |X_l|^2(X_{l+1} + X_{l-1}) = 0. \tag{3}$$

Equation (3) is a typical nonlinear differential-difference equation, it possesses an infinite number of conservation laws of motion E_m $\left(\frac{\mathrm{d}E_m}{\mathrm{d}s} = 0\right)$. Following Zakharov and Shabat [18], these laws can be constructed systematically from a scattering problem by considering asymptotic expansions (refer to Ablowitz and Ladik [1]).

Using some intermediate quantities $g_k^{(j)}$ ($j = 1, \ldots, 6$; $k = \ldots, -1, 0, 1, \ldots$) (as introduced in [1]), we give some program for fast calculation of E_m ($m = 1, \ldots, 6$) in a recursive manner:

$$-\overline{X}_k = \frac{g_{k+2}^{(1)}}{X_{k+1}}, \qquad 0 = \frac{g_{k+2}^{(2)}}{X_{k+1}} + X_k\frac{g_{k+1}^{(1)}}{X_k}\frac{g_{k+2}^{(1)}}{X_{k+1}} - \frac{g_{k+1}^{(1)}}{X_k},$$

$$0 = \frac{g_{k+2}^{(3)}}{X_{k+1}} + X_k\frac{g_{k+1}^{(1)}}{X_k}\frac{g_{k+2}^{(2)}}{X_{k+1}} + X_k\frac{g_{k+1}^{(2)}}{X_k}\frac{g_{k+2}^{(1)}}{X_{k+1}} - \frac{g_{k+1}^{(2)}}{X_k},$$

$$0 = \frac{g_{k+2}^{(4)}}{X_{k+1}} + X_k\frac{g_{k+1}^{(1)}}{X_k}\frac{g_{k+2}^{(3)}}{X_{k+1}} + X_k\frac{g_{k+1}^{(2)}}{X_k}\frac{g_{k+2}^{(2)}}{X_{k+1}} + X_k\frac{g_{k+1}^{(3)}}{X_k}\frac{g_{k+2}^{(1)}}{X_{k+1}} - \frac{g_{k+1}^{(3)}}{X_k},$$

$$0 = \frac{g_{k+2}^{(5)}}{X_{k+1}} + X_k\frac{g_{k+1}^{(1)}}{X_k}\frac{g_{k+2}^{(4)}}{X_{k+1}} + X_k\frac{g_{k+1}^{(2)}}{X_k}\frac{g_{k+2}^{(3)}}{X_{k+1}} + X_k\frac{g_{k+1}^{(3)}}{X_k}\frac{g_{k+2}^{(2)}}{X_{k+1}} + X_k\frac{g_{k+1}^{(4)}}{X_k}\frac{g_{k+2}^{(1)}}{X_{k+1}} - \frac{g_{k+1}^{(4)}}{X_k},$$

$$0 = \frac{g_{k+2}^{(6)}}{X_{k+1}} + X_k\frac{g_{k+1}^{(1)}}{X_k}\frac{g_{k+2}^{(5)}}{X_{k+1}} + X_k\frac{g_{k+1}^{(2)}}{X_k}\frac{g_{k+2}^{(4)}}{X_{k+1}} + X_k\frac{g_{k+1}^{(3)}}{X_k}\frac{g_{k+2}^{(3)}}{X_{k+1}} + X_k\frac{g_{k+1}^{(4)}}{X_k}\frac{g_{k+2}^{(2)}}{X_{k+1}} + X_k\frac{g_{k+1}^{(5)}}{X_k}\frac{g_{k+2}^{(1)}}{X_{k+1}} - \frac{g_{k+1}^{(5)}}{X_k}.$$

$$E_1 = -\sum_k g_k^{(1)}, \qquad E_2 = \sum_k \left\{\frac{1}{2}\left[g_k^{(1)}\right]^2 - g_k^{(2)}\right\},$$

$$E_3 = -\sum_k \left\{\frac{1}{3}\left[g_k^{(1)}\right]^3 - g_k^{(2)}g_k^{(1)} + g_k^{(3)}\right\}, \ldots.$$

We can write out their expansions as follows:

$$E_1 = \sum_k X_{k+1}\overline{X}_k, \qquad E_2 = \sum_k X_{k+1}^2\overline{X}_k^2 + 2\sum_k X_{k+1}\overline{X}_{k-1}U_k,$$

$$E_3 = \sum_k X_{k+1}^3\overline{X}_k^3 + 3\sum_k X_{k+1}^2\overline{X}_k\overline{X}_{k-1}U_k + 3\sum_k X_{k+1}X_k\overline{X}_{k-1}^2U_k + 3\sum_k X_{k+1}\overline{X}_{k-2}U_kU_{k-1},$$

$$\cdots\cdots\cdots\cdots$$

where $U_k = 1 + |X_k|^2$.

We will also test the evolution of $E_m = ER_m + \mathrm{i}EI_m$ (ER_m and EI_m are the real part and imaginary part of E_m, respectively), $1 \leqslant m \leqslant 6$ during numerical simulations in section 6.

4. Standardization of the A–L model

With isometric transformations $X_l = V_l \exp(2s\mathrm{i})$ and denotation $V_l = p_l + \mathrm{i}q_l, l = \ldots, -1, 0, 1, \ldots$, we rewrite (3) as

$$\mathrm{i}\frac{\mathrm{d}V_l}{\mathrm{d}s} = (1 + |V_l|^2)(V_{l+1} + V_{l-1}) \tag{4}$$

or the following general Hamiltonian system

$$\frac{\mathrm{d}}{\mathrm{d}s}Z = K^{-1}(Z)\nabla H(Z) \tag{5}$$

where $Z = [p^\top, q^\top]^\top$, and $p = [p_{-n}, \ldots, p_n]^\top$, $q = [q_{-n}, \ldots, q_n]^\top$;

$$K^{-1}(Z) = (k_{ij}(Z))_{(4n+2)\times(4n+2)} = \begin{bmatrix} O_{2n+1} & D \\ -D & O_{2n+1} \end{bmatrix} \tag{6}$$

is anti-symmetric, nondegenerate and satisfies

$$\frac{\partial k_{ab}(Z)}{\partial z_c} + \frac{\partial k_{bc}(Z)}{\partial z_a} + \frac{\partial k_{ca}(Z)}{\partial z_b} = 0, \qquad a, b, c = 1, \ldots, 4n+2,$$

$D = \mathrm{diag}\{U_{-n}, \ldots, U_n\}$, $U_l = 1 + p_l^2 + q_l^2$, $l = -n, \ldots, n$, O_{2n+1} is $(2n+1) \times (2n+1)$ null matrix; and

$$H(Z) = \sum_{l=-n}^{n} (p_l p_{l+1} + q_l q_{l+1}). \tag{7}$$

In the context of the Darboux theorem (see [2, 3]), (5) can be standardized. In fact for any general Hamiltonian system of the form (5), any transformation $\varphi : \mathbb{R}^{4n+2} \to \mathbb{R}^{4n+2}$, $\varphi(Y) = Z$ satisfying

$$\left[\frac{\partial \varphi}{\partial Y}\right]^\top K(\varphi(Y)) \left[\frac{\partial \varphi}{\partial Y}\right] = J \tag{8}$$

leads to a standard Hamiltonian system

$$\frac{\mathrm{d}}{\mathrm{d}s}Y = J^{-1}\nabla G(Y) \tag{9}$$

with $G(Y) = H \circ \varphi(Y)$, where $Y = [u^\top, v^\top]^\top$, $u = [u_{-n}, \ldots, u_n]^\top$, $v = [v_{-n}, \ldots, v_n]^\top$, $J = \left[\begin{smallmatrix} O_{2n+1} & I_{2n+1} \\ -I_{2n+1} & O_{2n+1} \end{smallmatrix}\right]$, I_{2n+1} is $(2n+1) \times (2n+1)$ identity matrix.

We note that in (6), $K^{-1}(Z)$ is completely splitable and so is $K(Z)$. Such being the special case, we can split the system in (8) into

$$\frac{\partial p_l}{\partial v_l}\frac{\partial q_l}{\partial u_l} - \frac{\partial q_l}{\partial v_l}\frac{\partial p_l}{\partial u_l} = U_l, \qquad l = -n, \ldots, n. \tag{10}$$

Now it becomes easy to find a coordinate transformation by solving equations in (10). We list several solutions ([17]) as follows.

Coordinate transformation **I**:

$$\begin{cases} p_l = \sqrt{1 + u_l^2}\tan\left(\sqrt{1 + u_l^2}v_l\right), \\ q_l = u_l, \qquad l = -n, \ldots, n \end{cases} \tag{11}$$

with inverse

$$\begin{cases} u_l = q_l, \\ v_l = \dfrac{\arctan\left(\frac{p_l}{\sqrt{1+q_l^2}}\right)}{\sqrt{1+q_l^2}}, \qquad l = -n, \ldots, n \end{cases} \tag{12}$$

and standard Hamiltonian

$$G(u, v) = \sum_{l=-n}^{n} \left\{ u_l u_{l+1} + \sqrt{1+u_l^2}\sqrt{1+u_{l+1}^2}\tan\left(\sqrt{1+u_l^2}v_l\right)\tan\left(\sqrt{1+u_{l+1}^2}v_{l+1}\right)\right\}. \tag{13}$$

Coordinate transformation **II**:

$$\begin{cases} p_l = \sqrt{\dfrac{\exp\left\{u_l^2+v_l^2\right\}-1}{u_l^2+v_l^2}}v_l, \\ q_l = \sqrt{\dfrac{\exp\left\{u_l^2+v_l^2\right\}-1}{u_l^2+v_l^2}}u_l, \qquad l = -n, \ldots, n \end{cases} \tag{14}$$

with inverse

$$\begin{cases} u_l = \sqrt{\dfrac{\ln\left(1+p_l^2+q_l^2\right)}{p_l^2+q_l^2}}q_l, \\ v_l = \sqrt{\dfrac{\ln\left(1+p_l^2+q_l^2\right)}{p_l^2+q_l^2}}p_l, \qquad l = -n, \ldots, n \end{cases} \tag{15}$$

and standard Hamiltonian

$$G(u, v) = \sum_{l=-n}^{n} \left\{ \sqrt{\frac{\exp\left\{u_l^2+v_l^2\right\}-1}{u_l^2+v_l^2}}\sqrt{\frac{\exp\left\{u_{l+1}^2+v_{l+1}^2\right\}-1}{u_{l+1}^2+v_{l+1}^2}}(u_l u_{l+1}+v_l v_{l+1}) \right\}. \tag{16}$$

Coordinate transformation **III**:

$$\begin{cases} p_l = \sqrt{\exp v_l - 1}\cos(2u_l), \\ q_l = \sqrt{\exp v_l - 1}\sin(2u_l), \qquad l = -n, \ldots, n \end{cases} \tag{17}$$

with inverse

$$\begin{cases} u_l = \dfrac{1}{2}\arctan\dfrac{q_l}{p_l}, \\ v_l = \ln\left(1+p_l^2+q_l^2\right), \qquad l = -n, \ldots, n \end{cases} \tag{18}$$

and standard Hamiltonian

$$G(u, v) = \sum_{l=-n}^{n} \sqrt{(\exp v_l - 1)(\exp v_{l+1} - 1)}\cos(2[u_l - u_{l+1}]). \tag{19}$$

Coordinate transformation **I** has been successfully used to deal with the A–L model by Tang, Pérez-García and Vázquez [16]. They simulated the solitons motion and tested the evolution of the first three discrete invariants of the A–L model. As suggested by Hairer, Lubich and Wanner [8], coordinate transformation **II** treats the variables more symmetrically. This symmetry may improve the numerical results obtained by using coordinate transformation **I**. Coordinate transformation **III** may bring some difficulty to numerical simulation, due to the illness of u_l depending on p_l in (18) and the derivatives of G with respect to v_l in (19), $l = -n, \ldots, n$.

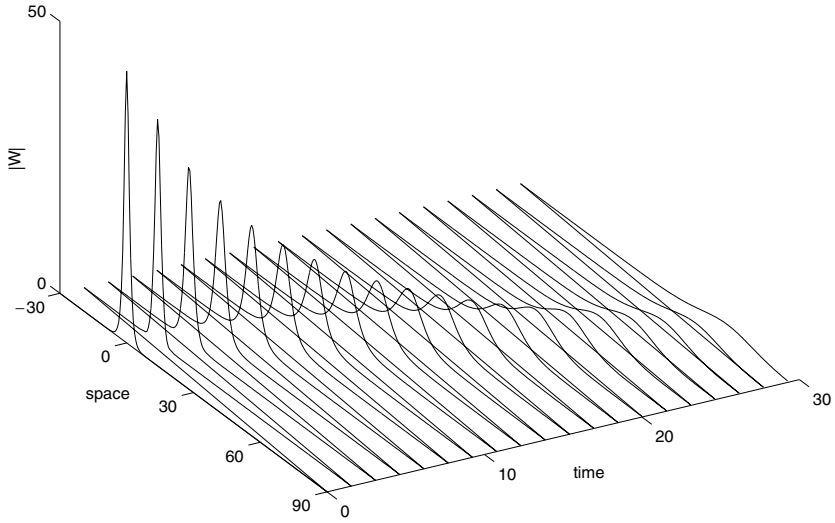

Figure 1. Single soliton motion computed by using scheme **S2** to (4).

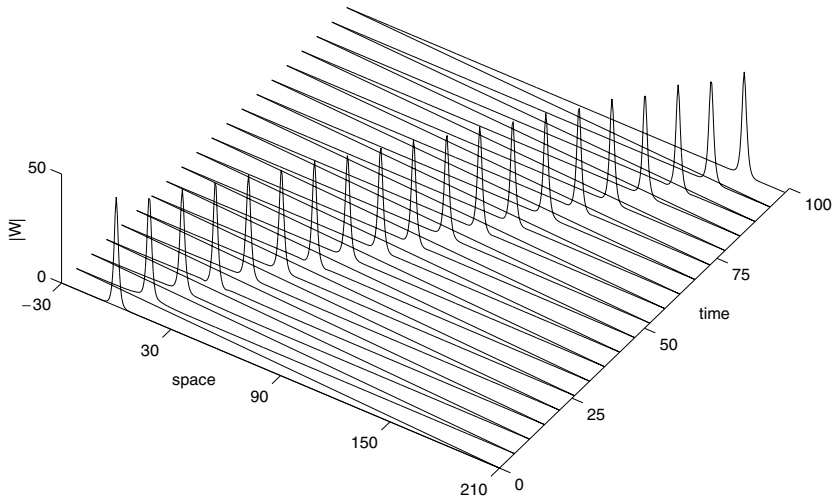

Figure 2. Single soliton motion computed by using scheme **S1** to (9) with (13).

5. Symplectic and non-symplectic schemes

Since the A–L model (2) has already been changed into a standard Hamiltonian system, we can use the usual symplectic schemes (see [4, 6, 8, 13] for an introduction to symplectic numerical methods for Hamiltonian dynamics) straightforward. In comparison with the symplectic methods, we will also use a non-symplectic scheme directly to the A–L model.

Scheme 1 (**S1**): *the midpoint rule*.

$$\widetilde{Z} = Z + \tau f\left(\frac{\widetilde{Z} + Z}{2}\right) \tag{20}$$

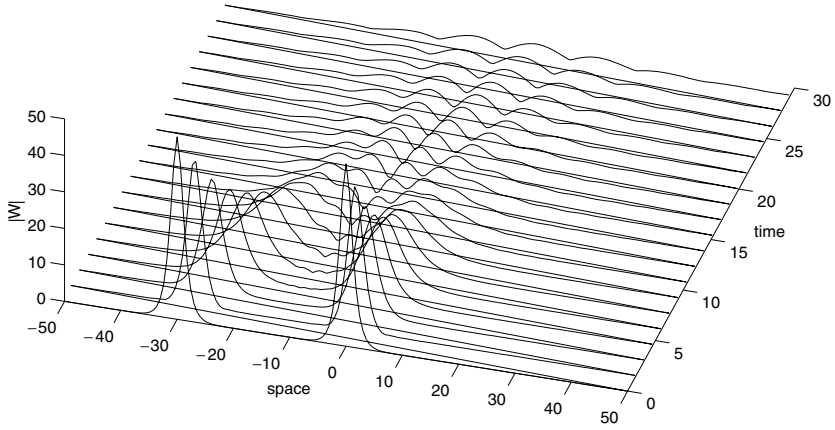

Figure 3. Propagation of two solitons computed by using scheme **S2** to (4).

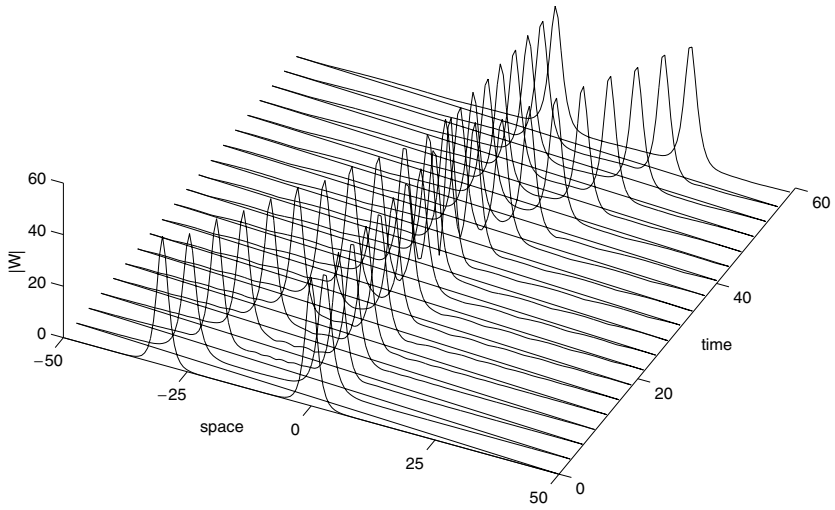

Figure 4. Propagation of two solitons computed by using scheme **S1** to (9) with (13).

where τ is the temporal step-size. The scheme **S1** is of second order, revertible in τ. And it is symplectic for standard Hamiltonian systems ($f = J^{-1}\nabla H$), and preserves any quadratic invariants of the Hamiltonian H (see [7]).

Scheme 2 (**S2**): *third-order scheme*.

$$\begin{cases} \widetilde{Z} = Z + \dfrac{\tau}{2}[f(K_1) + f(K_2)], \\ K_1 = Z + \dfrac{\tau}{6}[3f(K_1) - \sqrt{3}f(K_2)], \\ K_2 = Z + \dfrac{\tau}{6}[\sqrt{3}f(K_1) + 3f(K_2)]. \end{cases} \tag{21}$$

This Runge–Kutta scheme is of third order but non-symplectic for standard Hamiltonian systems.

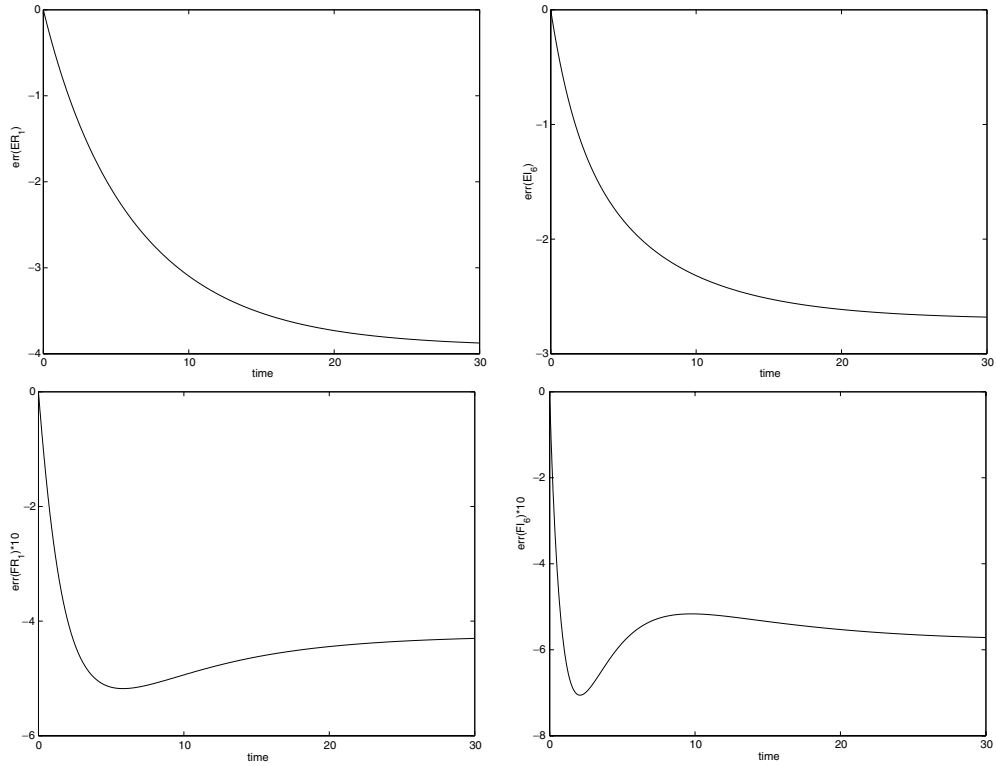

Figure 5. Evolution of ER_1, EI_6, FR_1 and FI_6 obtained by using scheme **S2** to (4).

6. Numerical experiments

In this section, we will present the numerical simulation results performed in order to test the accuracy of the symplectic scheme and its conservativity of invariants or approximations in comparison with the non-symplectic scheme, and show the differences between the numerical results of the same symplectic scheme applied to different standardized Hamiltonians.

The following initial conditions are used.

Condition 1: one-soliton solution.

$$W(x,0) = 2\eta\sqrt{\frac{2}{a}}\,\mathrm{e}^{2\chi x i}\,\mathrm{sech}[2\eta(x-x_1)]. \tag{22}$$

Condition 2: two-soliton solution.

$$W(x,0) = 2\eta_1\sqrt{\frac{2}{a}}\,\mathrm{e}^{2\chi_1 x\mathrm{i}}\mathrm{sech}[2\eta_1(x-x_a)] + 2\eta_2\sqrt{\frac{2}{a}}\,\mathrm{e}^{2\chi_2 x\mathrm{i}}\mathrm{sech}[2\eta_2(x-x_b)]. \tag{23}$$

Condition 3: three-soliton solution.

$$W(x,0) = \mathrm{sech}[x-x_3]. \tag{24}$$

Unless the contrary is stated the standard value for the nonlinear constant is $a = 2.0$.

We will apply the symplectic method **S1** to (9) with Hamiltonian functions (13), (16) or (19), and the non-symplectic scheme **S2** to (4).

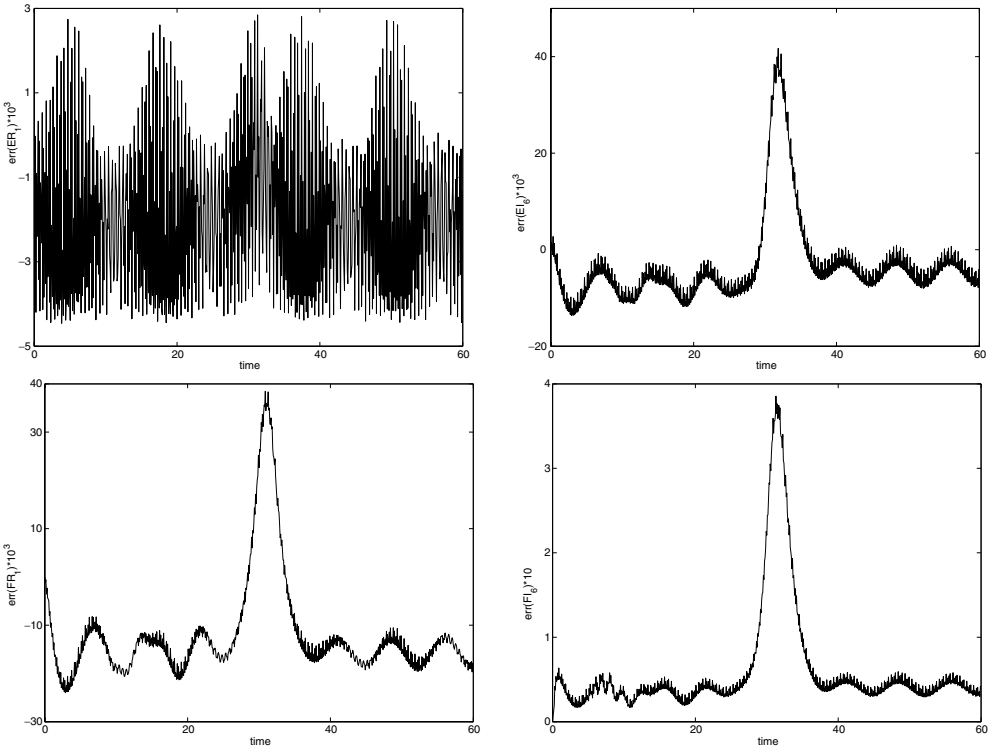

Figure 6. Evolution of ER_1, EI_6, FR_1 and FI_6 obtained by using scheme **S1** to (9) with (13).

In the following, we will call $\mathrm{err}(A)(t) = A(t) - A(0)$ for any variable A.

Initial data (22) are the usual 1-soliton solution which are integrated without problems by many numerical methods. We present here the results of an integration with $\eta = 0.5$, $\chi = 0.5$, $x_1 = 0.0$ over the spatial interval $x \in [-750, 750]$ and temporal intervals $0 \leqslant t \leqslant 100$ for symplectic and non-symplectic method, with same integration parameters:

$$h = 0.3, \quad \tau = 0.02.$$

In figures 1 and 2, we find that the symplectic scheme can simulate the single soliton motion successfully, and the non-symplectic method cannot do even in a shorter interval $0 \leqslant t \leqslant 30$.

The expression in (23) is initial data for a pair of solitons with different amplitudes and velocities and it is appropriate for the simulation of soliton collision (assuming that the soliton centres are initially set far away from each other). We have studied the following set of parameters $\eta_1 = \eta_2 = 0.5$, $\chi_1 = 0.25$, $\chi_2 = 0.025$, $x_a = 30.0$, $x_b = 0.0$ and

$$h = 0.3, \quad \tau = 0.02.$$

Figures 3 and 4 show again the advantage of symplectic methods in preserving the motions of two solitons.

Since the evolution of other ER_j, EI_k, FR_l and FI_m is very similar, we plot only $\mathrm{err}(ER_1)$, $\mathrm{err}(EI_6)$, $\mathrm{err}(FR_1)$ and $\mathrm{err}(FI_6)$ in figures 5, 6, 7 respectively. Figures 6 and 7 show that the numerical results for the invariants of the A–L model and the approximations to the conserved quantities of the original NLSE obtained by using symplectic scheme **S1** always undulate in small neighbuorhoods of the standard values respectively, while figure 5

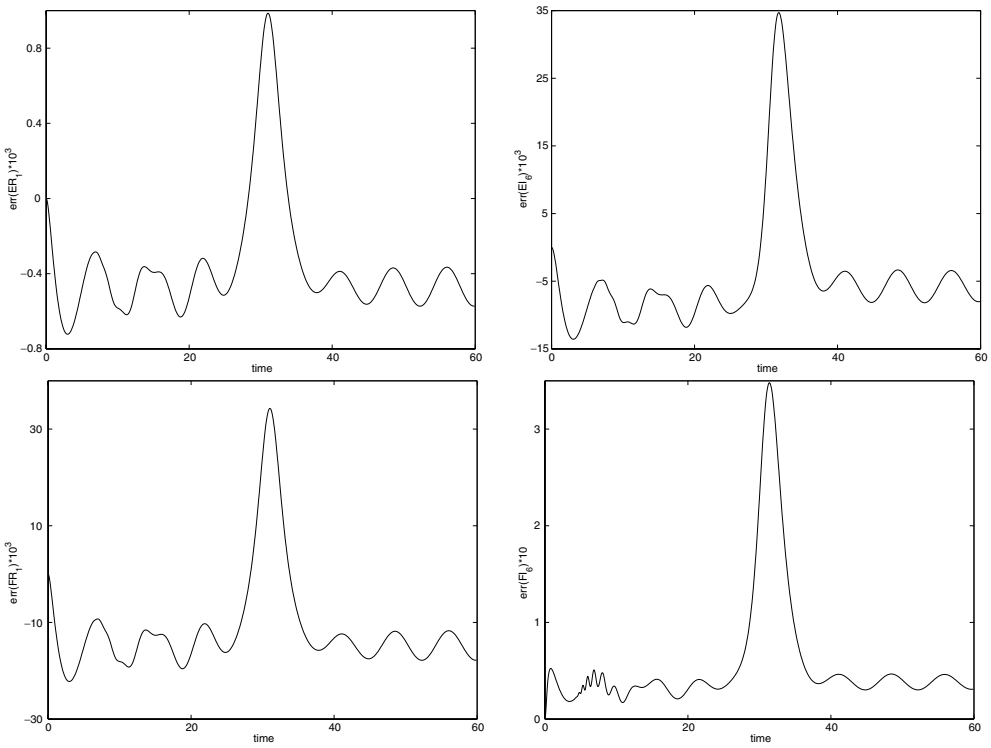

Figure 7. Evolution of ER_1, EI_6, FR_1 and FI_6 obtained by using scheme **S1** to (9) with (16).

shows that the corresponding numerical results obtained by using non-symplectic scheme **S2** degenerate with time. These phenomena are in good agreement with the solitons motion plotted in figures 3 and 4, respectively.

Though the behaviour of invariants and approximations presented in both figures 6 and 7 is qualitatively good, one still easily finds the difference between these two figures. The plots in figure 7 seem to be much more 'clean' than those in figure 6. In this sense one may say that it is the symmetry of coordinate transformation **II** (for simplicity, C–T **II**) that improves the computation results obtained by using coordinate transformation **I** (for simplicity, C–T **I**). On the other hand, We need to point out that the implementation procedure for C–T **II** is more complicated than that for C–T **I**, because of the appearance of exponential function.

Numerical experiments show that the Hamiltonian system (9) given by (19) is not numerically integrable by the schemes **S1** or other higher order symplectic methods. Running of the Fortran program can last only several temporal steps no matter how small the step-size is chosen, because of the appearance of 'DOMAIN error in sqrt'.

Numerical experiments show that the numerical results obtained by using the non-symplectic scheme **S2** to the Hamiltonian system (9) given by (13) or by (16) are very similar to those obtained by using **S2** directly to (4); and obviously the simulation process of the former is more time-consuming than that of the latter.

Finally, we have used the initial data (24), which is usually considered to be a more difficult 'quality' test for numerical schemes because of the appearance of large spatial and temporal gradients in the solution. For $a = 2N^2 (N = 2, 3, \ldots)$ Miles has shown that (24) corresponds to a bounded state of N solitons [12]. For the case $a = 18$, we found that for

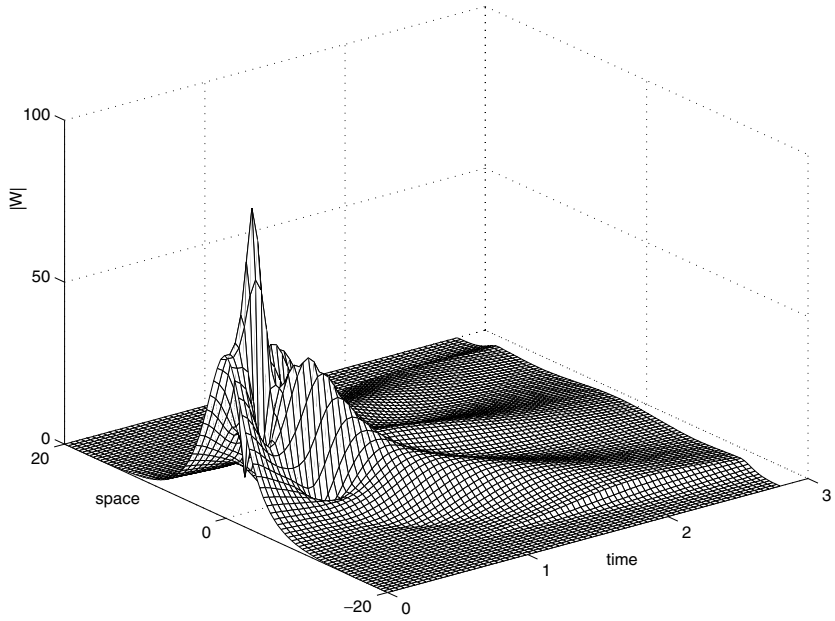

Figure 8. Propagation of three-soliton bounded state computed by using scheme **S2** to (4).

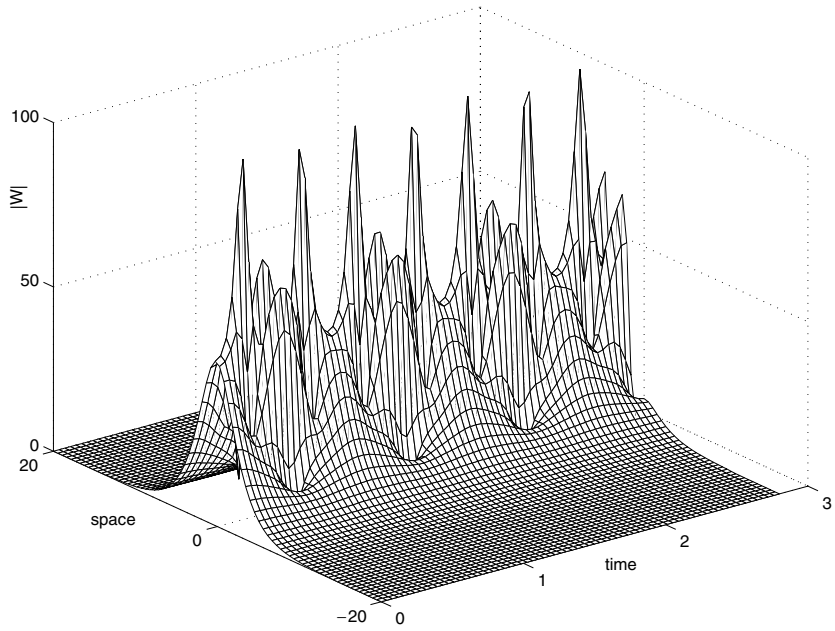

Figure 9. Propagation of three-soliton bounded state computed by using scheme **S1** to (9) with (13).

$h \leqslant 0.06667$, with some proper temporal step-size which makes simple iteration practicable, the second-order symplectic scheme **S1** represents accurately the solution without problems (figure 9 where $x_3 = 0.0$). This is a very good result and provides convergence to the correct

solution with a relatively rough spatial grid, while the third-order non-symplectic scheme **S2** studied for comparison fails to do so (figure 8).

7. Concluding remarks

The Ablowitz–Ladik model of the nonlinear Schrödinger equation is a completely integrable general Hamiltonian system which can be standardized via coordinate transformations. When a suitable coordinate transformation is chosen, the symplectic method applied to the standardized Hamiltonian system has overwhelming superiorities over the non-symplectic scheme applied directly to the A–L model, such as long-term tracking of solitons motion, long-term preserving of discrete invariants of the A–L model and also the conserved quantities of the original NLSE up to a very small error. The difference between the numerical results obtained via different coordinate transformations shows the importance of symmetry for choosing a coordinate transformation in our procedure.

On the other hand, the main disadvantage of this method (Ablowitz–Ladik+coordinate transformation+symplectic integration, simply, ALCTSI) is that due to the complexity of the standardized Hamiltonian, we have to use iterative methods to solve the highly nonlinear system. This fact makes the implementation process time-consuming when compared with spectral methods [15] or linearly implicit finite difference schemes [19] which are commonly used to integrate the NLSE. When noncritical problems are considered, it is a thing to choose a scheme; but for more difficult or complicated problems, the additional guaranties provided by ALCTSI may be of high interest, and in any case this method provides a safe way to check the results of the faster but less accurate methods when typical physical problems are to be studied.

Acknowledgments

We would like to thank the referees for their valuable suggestions that greatly helped us to improve the paper. This research is supported by the 'Informatization Construction of Knowledge Innovation' Projects of the Chinese Academy of Sciences 'Supercomputing Environment Construction and Application' (INF105-SCE), and by National Natural Science Foundation of China (grant no. 10471145), and by Morningside Center of Mathematics, Chinese Academy of Sciences.

References

[1] Ablowitz M J and Ladik J F 1976 Nonlinear differential-difference equations and Fourier analysis *J. Math. Phys.* **17** 1011–8
[2] Abraham R E and Marsden J E 1978 *Foundations of Mechanics* (Reading, MA: Benjamin-Cummings)
[3] Arnold V I 1978 *Mathematical Methods of Classical Mechanics* (New York: Springer)
[4] Channell P J and Scovel J C 1990 Symplectic integration of Hamiltonian systems *Nonlinearity* **3** 231–59
[5] Dodd R K, Eibeck J C, Gibbon J D and Morris H C 1982 *Solitons and Nonlinear Wave Equation* (New York: Academic)
[6] Feng K 1985 *On Difference Schemes and Symplectic Geometry: Proc. 1984 Beijing Symposium on Differential Geometry and Differential Equations* ed K Feng (Beijing: Science) pp 42–58
[7] Ge Z and Feng K 1988 On the approximation of linear Hamiltonian systems *J. Comput. Math.* **6** 88–97
[8] Hairer E, Lubich Ch and Wanner G 2002 *Geometric Numerical Integration* (Berlin: Springer)
[9] Hasegawa A 1989 *Optical Solitons in Fibers* (Berlin: Springer)
[10] Herbst B M, Varadi F and Ablowitz M J 1994 Symplectic methods for the nonlinear Schrödinger equation *Math. Comput. Simul.* **37** 353–69
[11] Konotop V V and Vázquez L 1994 *Nonlinear Random Waves* (Singapore: World Scientific)

[12] Miles J W 1981 An envelope soliton problem *SIAM J. Appl. Math.* **41** 227–30
[13] Sanz-Serna J M and Calvo M P 1994 *Numerical Hamiltonian Problems* (London: Chapman and Hall)
[14] Schober C M 1999 Symplectic integrators for the Ablowitz–Ladik discrete nonlinear Schrödinger equation *Phys. Lett.* A **259** 140–51
[15] Taha T R and Ablowitz M 1984 Analytical and numerical aspects of certain nonlinear evolution equations: II. Numerical, nonlinear Schrödinger equation *J. Comput. Phys.* **55** 203–30
[16] Tang Y F, Pérez-García V M and Vázquez L 1997 Symplectic methods for the Ablowitz–Ladik *Appl. Math. Comput.* **82** 17–38
[17] Tang Y F 1997 Standardization of the Ablowitz–Ladik model as a Hamiltonian system *Research Reprot 1997-006 of ICMSEC, CAS* unpublished
[18] Zakharov V E and Shabat A B 1973 Interaction between solitions in a stable medium *Sov. Phys.—JETP* **37** 823–8
[19] Zhang F, Pérez-García V M and Vázquez L 1995 Numerical simulation of nonlinear Schrödionger systems: a new conservative scheme *Appl. Math. Comput.* **71** 165–77